

IKFlow: Generating Diverse Inverse Kinematics Solutions

Barrett Ames^{*1}

Jeremy Morgan^{*2}

George Konidaris³

Abstract—Inverse kinematics—finding joint poses that reach a given Cartesian-space end-effector pose—is a common operation in robotics, since goals and waypoints are typically defined in Cartesian space, but robots must be controlled in joint space. However, existing inverse kinematics solvers return a single solution pose, where systems with more than 6 degrees of freedom support infinitely many such solutions, which can be useful in the presence of constraints, pose preferences, or obstacles. We introduce a method that uses a deep neural network to learn to generate a diverse set of samples from the solution space of such kinematic chains. The resulting samples can be generated quickly (2000 solutions in under 10ms) and accurately (to within 10 millimeters and 2 degrees of an exact solution) and can be rapidly refined by classical methods if necessary.

I. INTRODUCTION

Inverse Kinematics (IK) maps a task-space Cartesian pose to a set of joint space angles, which is a critically important operation for several reasons. For example, it is typically easier to define tasks in a specialized Cartesian coordinate frame that is easily interpretable by the robot’s operator— more concretely, specifying a curve to draw on a whiteboard is easier in the frame of the whiteboard. Similarly, it is beneficial to express the grasp pose in Cartesian space, allowing for a robot to plan to a multitude of valid joint space poses. Of course, each Cartesian-space goal must be translated to a joint pose for the robot to control to; therefore, these scenarios are only possible with a fast IK solver.

Although there are several open source IK packages [3, 18, 6], their functionality is still incomplete. Analytical solvers like IKFast and IKBT [18] are fast and return all the solutions for an arm, but cannot be applied to arms with more than 6 degrees of freedom (DOF). Numerical solvers can be applied to arms with any number of joints, but only return a single solution, if one is found at all. A solver that can provide many solutions for an arm with 7-DOF or greater, and do so quickly, would enable several new applications.

One such application is generating motion plans, which in theory could be performed quickly and robustly for arms with more than 6 DOFs. First, an optimal Cartesian path of a robot’s end effector, starting at its current pose and ending at the target pose, would be found through heuristic driven search. The solver would then provide a dense and diverse set of joint poses along this optimal path. A planner would then search through these joint poses to efficiently create a motion plan through the robots configuration space.

For a second application, solution space samples can be used to infer properties about the solution space. This would

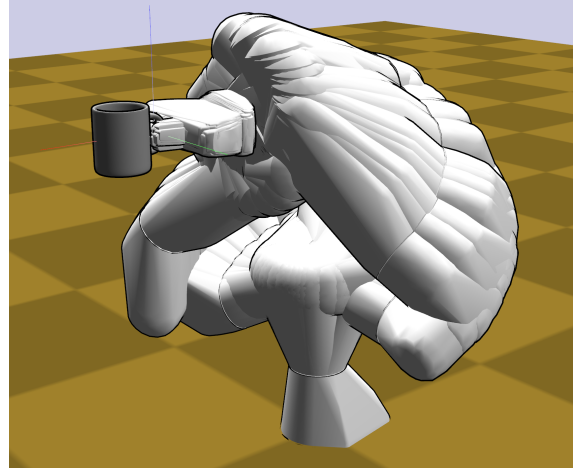


Fig. 1: One hundred approximate solutions generated by IKFlow, for a Panda arm reaching to a given end-effector pose.

allow for a form of sampling based kinematic analysis to occur quickly. An example of this is illustrated by a robot with two Cartesian paths it can follow. IKFlow could be used to assess the qualities of the solution spaces along the two paths. For example, if one path has a solution space with more volume than the other it may be preferred because it can better respond to new obstacles.

An ideal 7+ DOF IK solver should return a set of solutions that approximately cover the entire solution set; these samples should be near-exact solutions. Additionally, it should do so quickly, if it is to serve as a primitive usable in the inner loop of higher-level control algorithms. Of these three requirements, accuracy is the least important because the forward kinematics operation is very fast, so verifying a sample is efficient, and numerical IK solvers can be seeded with an approximate solution to rapidly refine it to any desired accuracy.

We propose IKFlow, a new IK method that satisfies these requirements by training a neural network to output a diverse set of poses that approximately satisfy a given Cartesian goal pose. By viewing the problem as generative modeling over the solution space, we are able to exploit recent advances in a Normalizing Flows [16], a new generative modeling approach capable of modeling multi-modal distributions with nonlinear interactions between variables. We show, using several different humanoid robot models, that IKFlow can be trained—once off, per-robot—to rapidly generate hundreds to thousands of diverse approximate solutions; we also provide a practical open-source implementation of our approach.

^{*}, equal contribution

¹Duke University Computer Science, cbames@cs.duke.edu

²Third Wave Automation, jeremy@thirdwave.ai

³Brown University Computer Science, gdk@cs.brown.edu

II. BACKGROUND AND RELATED WORK

A. Inverse Kinematics (IK)

Inverse Kinematics defines the mapping from a robot’s operational space to its joint space:

$$f : P \rightarrow T^n,$$

where n is the number of joints. The topology of the joint space is the n -dimensional torus, $T^n = S^1 \times S^1 \dots \times S^1$. The topology of P is determined by the workspace of the robot, but we focus on the case where the end effector pose is in $P := SE(3)$. If the robot has joint limits then the topology of the mapping changes:

$$f : P \rightarrow R^n,$$

where R^n is the n -dimensional Euclidean space. This topological difference is important because it allows for many robots to be modeled by generic density estimators, instead of special purpose estimators built for tori [17]. In the case that the degrees of freedom of the robot exceed the degrees of freedom of the operational space (i.e. the robot is kinematically redundant) there are infinitely many solutions. This occurs because the extra degree of freedom allows for a continuum of configurations that satisfy the desired Cartesian goal. In this situation the best and only solution is to provide a description of the solution space that can extract relevant features for the application. Thus for a specific pose $p \in SE(3)$ an IK solver should return a subset of joint space:

$$f : p \rightarrow R_g^n \subseteq R^n.$$

Existing solutions for describing this solution space fall into two categories. The first category uses only a single point to describe the solution space, but returns quickly, on the order of 0.1 millisecond. The second approach returns a more thorough set of solution points, but requires extensive random sampling, and thus is significantly slower, on the order of seconds for thousands of solutions. The approach we detail in Section III uses generative modeling to generate upwards of a thousand solutions in under 10 milliseconds.

B. Related Work

There have been a number of attempts to use neural networks for inverse kinematics [5, 15, 7, 1]. Most of these approaches do not solely implement the inverse kinematics function. For example, Csiszar et al. incorporate the problem of calibrating the physical robot with its internal model. Ren and Ben-Tzvi incorporate the dynamics of the robot. Almusawi et al. learn the kinematics model in addition to performing Cartesian control. Demby’S et al. do create a neural network approach that focuses exclusively on the IK problem, but conclude that it is not a fruitful path.

Fundamentally, the architectures used in the previous approaches are all limited as they are only capable of returning a single solution for a particular input. However, IK is a one-to-many mapping, and access to additional solutions may prove useful for the control layer above IK. Ardizzone et al. apply a

similar deep generative approach to IKFlow but only a small planar IK problem. We extend and refine their work in three key ways. First, we decrease the amount of error present in the solutions. Second, we improve training stability by addressing a corner case related to the dimensionality of solution spaces. Third, we expand the coverage to include the entire physical workspace of the arm.

C. Deep Generative Modeling

Generative modeling represents arbitrary distributions in such a way that they can be sampled. This is achieved by transforming known base distributions into target distributions. For example:

$$g : N(\hat{0}, I) \rightarrow Q,$$

where Q is an arbitrary distribution and g is a neural network. We draw samples from the arbitrary distribution by drawing samples from the base distribution and passing them through g . There are several different methods for performing generative modeling. We selected our approach based on the following criteria. First, the diversity of samples returned is important to ensure that the full breadth of the solution space is returned. Second, the approach must be able to handle multi-modal data and nonlinear dependencies between variables in order to cover the solution space. Third, the method must be capable of handling conditional information, because the solution space is conditioned on the Cartesian goal. Fourth, the method must sample solutions quickly because IK is often used as a primitive by other procedures. Finally, the sampling procedure must produce samples with high accuracy. Given these desired properties we propose to use a normalizing flow approach.

1) *Normalizing Flows*: Normalizing Flows are a generative modeling approach that relies on two important components. The first component is a series of functions that are easy to invert. These easily invertible functions enable the same network to quickly estimate densities and produce samples. In the literature, this series of functions is commonly referred to as the *coupling layers*. Sampling is performed by passing a sample from the base distribution through each of the coupling layers:

$$\hat{x} = f_1 \circ f_2 \dots \circ f_n(\hat{z}), \hat{z} \sim N(\hat{0}, I), \quad (1)$$

where \hat{x} is the sample in the data space and \hat{z} is a sample from the base distribution. The second important component is the efficient calculation of the Jacobian’s determinant. This enables density estimation of a data point to be computed with the change of variables formula:

$$p_X(\hat{x}) = p_Z(\hat{z}) \left| \det \left(\frac{\partial g(\hat{z})}{\partial \hat{z}^T} \right) \right|^{-1}.$$

The change of variables formula allows a distribution over one set of variables to be described by another set of variables given the determinant of the Jacobian between the two variables. A normalizing flow uses this along with a simple prior distribution, $p(z)$ —here a Normal distribution—to enable density estimation of the data distribution $p(x)$. To make the determinant of the Jacobian tractable, special coupling layers

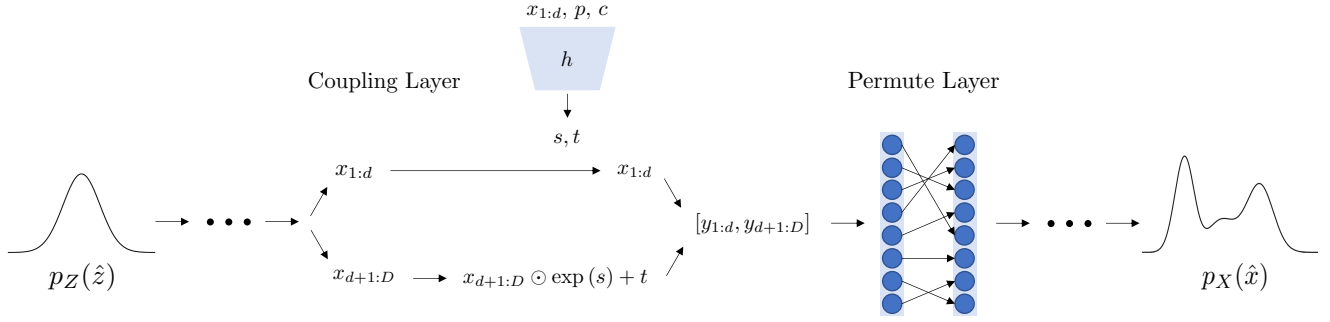


Fig. 2: The basic architecture of a conditional normalizing flow network. The base distribution sample is fed into a coupling layer. The coupling layer contains a coefficient network which transforms a subset of the sample. The permutation changes the order of the samples so that the coefficient network of the next coupling layer affects a different subset of the sample. Conditional information is passed into every coupling layer.

are used [9, 12, 8]. The coupling layer we use was developed by Kingma and Dhariwal:

$$y_{1:d} = x_{1:d} \quad (2)$$

$$s, t = h(x_{1:d}) \quad (3)$$

$$y_{d+1:D} = x_{d+1:D} \odot \exp(s) + t, \quad (4)$$

where x is the input data to a layer, and y is the output. s affects the scaling of the layer, and t shifts the input of the layer. This layer is then inverted by:

$$x_{1:d} = y_{1:d}$$

$$s, t = h(x_{1:d})$$

$$x_{d+1:D} = (y_{d+1:D} - t) \odot \exp(-s).$$

An important property of the layers is that they can be inverted without inverting the function h that produces s and t . h , also known as the coefficient network, can therefore be arbitrarily complex. Further, by holding $\hat{x}_{1:d}$ constant through the transformation, the Jacobian will have zeros in the upper diagonal, and thus the determinant will only be the product of the diagonals of the Jacobian.

2) *Conditional Normalizing Flows*: Conditional Normalizing Flows change the scaling and shifting of a coupling layer based on conditional information. The conditional information, c , is passed as part of the input to the network which estimates s and t . Now h is a function of both $x_{1:d}$ and c . The invertibility of the coupling layer remains unaffected because the conditioning information is passed into h which need not be inverted to invert the layer. Figure 2 provides a simple diagram of the architecture. While other methods have been proposed for conditioning normalizing flows (i.e. Arditzone et al.) this formulation reduces the number of hyperparameters that must be tuned, and has a simple Maximum Likelihood training loss:

$$\mathcal{L} = -\log(p_Z(z)) - \log \left| \det \left(\frac{\partial g(z|c)}{\partial z^T} \right) \right|^{-1}. \quad (5)$$

For a more thorough review of Normalizing Flows see Papamakarios et al..

3) *Maximum Mean Discrepancy (MMD)*: Finally, a method for comparing distributions is necessary to evaluate the performance of a generative model. We use Maximum Mean Discrepancy (MMD) because of its strong theoretical properties and ease of implementation. Given two distributions, $P(X)$ and $Q(Y)$, MMD computes the distance between the two distributions as the squared distance between the mean of the embeddings of the distributions.

$$\text{MMD}(P, Q) = \|E_{X \sim P}[\phi(X)] - E_{Y \sim Q}[\phi(Y)]\|.$$

Notably, the embeddings must be in a Reproducing Kernel Hilbert Space (RKHS). The capability of MMD to capture the distance between two distributions is dependent on the selection of a good embedding function ϕ . We selected the inverse multi-quadric kernel because of its long tails and previous use [2]. A more detailed analysis of Maximum Mean Discrepancy is provided by Gretton et al..

III. IKFLOW: LEARNED INVERSE KINEMATICS

The first step to learning inverse kinematics is to treat the solution space as a distribution that has a uniform probability, may be multi-modal, and is conditioned on the desired pose. We model the solution distribution with Conditional Normalizing Flows because they are fast to train and sample and can handle the complexity of the solution distributions. There are three steps to applying Conditional Normalizing Flows to the inverse kinematics problem. First, a data set must be constructed. Second, we must select an architecture and parameters of the architecture. Third, we must design a loss function for minimizing the difference between samples from the generative model and the data distribution.

A. Data Generation

One advantage of the inverse kinematics problem is the relative ease with which data can be generated. All serial kinematic chains have known forward kinematics that can be used to generate training data. Data is generated by uniformly sampling from the interval defined by the joint limits. The joint samples are then fed through a forward kinematics function to

Robot	DOF	Coupling Layer Width	Coupling Layers
ATLAS (2013) - Arm and Waist	9	15	9
ATLAS (2013) - Arm and Waist	6	15	12
Panda	7	9	12
Robonaut 2 - Arm and Waist	8	15	12
Robonaut 2 - Arm	7	15	12
Valkyrie - Whole Arm and Waist	10	15	16
Valkyrie - Lower Arm	4	15	9
Valkyrie - Whole Arm	7	15	12

TABLE I: The primary parameter to select when fitting a network to a new kinematic chain is the number of coupling layers. The number of coupling layers increases the expressivity of the invertible portion of the network. The network can also be made more expressive by increasing the coupling layer width. When the width becomes larger than the DOF the system becomes more capable of representing multi-modal target distributions.

obtain the corresponding Cartesian pose. The Cartesian pose becomes the conditional input to the network and the joint data is used as the target distribution. More sophisticated sampling methods could be used to account for effects at joint limits and for self-collisions, but we were able to obtain satisfactory performance without them. We leave this investigation for future work.

B. Normalizing Flow Architecture

The fundamental architecture of the network is defined by the use of normalizing flows, and was detailed in equations 1-4. The remaining design choices include the selection of a base distribution, selecting the number of coupling layers, the width of each coupling layer, and specification of the coefficient network.

The base distribution affects the complexity of the density estimation and the sampling speed. We chose the Normal distribution because it simplifies the calculation of the Maximum Likelihood Loss function and is quick to sample. The remaining choices for the architecture affect the capability of the network to fit a target distribution. The width of each coupling layer must be at least as large as the degrees of freedom; if it is larger than the DOF it allows for multi-modal distributions to be more easily modeled. The number of coupling layers required depends on the interactions of joints with each other. The more complex the inter-joint relationship, the more coupling layers are required, as more layers allow for more interaction between joints because of the permutation layers.

Finally, the coefficient network must be expressive enough to capture dependencies between the conditional information (i.e. the goal pose) and a subset of the layer values. Table I details the variable parameters (selected by hyperparameter search) for each kinematic chain that we test.

C. Loss Functions

The Maximum Likelihood loss detailed in equation 5 is theoretically the only loss function necessary for achieving high performance. However, for several of the kinematic chains tested, training diverged when trained with the Maximum Likelihood loss. The cause of this divergence was a mismatch between the dimension of the solution manifolds and the base distribution.

1) *Solution Sub-manifolds:* In Figure 3a the last joint of the arm appears in only one position. This implies that the solution space of that particular pose is not the same dimension as the joint space, because only 6 of the 7 joints in the arm can vary. This is not a unique situation, but occurs throughout the configuration space as some Cartesian poses can only be reached by fixing one of the joints at a specific configuration, for example at one of its limits. This is problematic because the normalizing flow approach does not perform well on distributions that are lower dimension than the base distribution. More specifically the change of variables equation (II-C1) does not hold if the base distribution and the target distribution are not the same dimension. One way to ensure the target distribution and the base distribution are the same dimension is to add noise that is the full dimension [11]. If the magnitude of the added noise is passed in as a conditional variable, its effect can be removed at test time by setting that piece of the conditional to 0:

$$\begin{aligned} c &\sim U(0, 1) \\ v &\sim N(0, c) \\ \hat{x} &= x + v, \end{aligned}$$

where c and v are drawn every training iteration, and added to the training data. The resulting loss function is:

$$\mathcal{L} = -\log(p_Z(z)) - \log \left| \det \left(\frac{\partial g(z|p, c)}{\partial z^T} \right) \right|^{-1}, \quad (6)$$

where p is the desired Cartesian pose.

IV. EXPERIMENTS

Models were built with the FrEIA framework [2] and trained with PyTorch [14]. Training performance was managed using Weights and Biases [4]. Additional details about the network architectures and training parameters can be found in the appendix.

Once trained the model was evaluated on the three desired quantities: speed, accuracy, and solution space coverage. Speed was measured by the time required to sample 100 solutions for a given Cartesian Pose, averaged over 50 randomly-generated poses. In addition, to understand how the model scales, runtime was measured as the number of requested solutions increased.

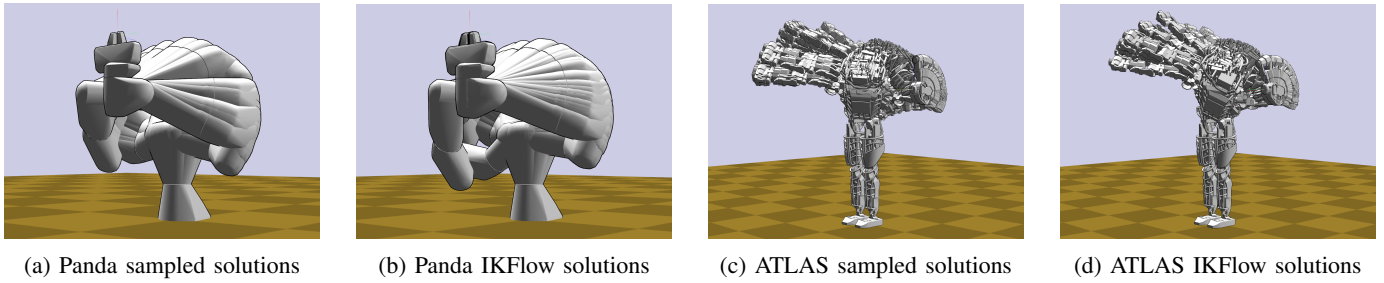


Fig. 3: A comparison of samples created by rejection sampling and samples from IKFlow for two robots, the Panda arm and ATLAS. Qualitatively, the solutions returned by the IKFlow models look to cover the same space of solutions found through rejection sampling. The MMD score between the two Panda solutions is 0.0122. The MMD score between the ATLAS solutions is 0.0081.

Model accuracy was measured by sampling 1000 test Cartesian poses and obtaining 100 joint solutions for each Cartesian pose. The joint solutions were then passed into a forward kinematics routine to compute the realized Cartesian pose. The averaged difference between the desired and the realized pose was recorded.

The MMD Score is found by taking the average of 1000 Maximum Mean Discrepancy scores, each calculated between sets of solutions returned by a rejection sampling approach, and by IKFlow. For each calculation, 250 samples are generated by each method for a randomly drawn pose. Lower values of MMD imply the distributions are more similar; thus when the IKFlow achieves a low MMD score, it provides good coverage of the solution space. These experiments were carried out on 8 different kinematic chains across 4 different robots, to evaluate the generality of the approach across different kinematic structures.

V. RESULTS

Our results show that our approach provides a representative set of solutions, quickly, with acceptable error. The results of all the experiments can be found in Table II.

A. Accuracy

The accuracy of the system output ranges from 6.3mm to 0.4mm and from 2.8 degrees to 0.15 degrees. For a point of reference, the mechanical repeatability of many industrial arms is 0.1mm. This level of accuracy is sufficient for many tasks; additionally these solutions can also be refined with numerical optimization approaches to reach arbitrary levels of precision. The refinement is quick (under 0.1 ms) because of the proximity of the seed to the solution.

B. Runtime

The runtime of the approach is fast enough to enable its use as a sub-routine in other algorithms. Nonlinear optimization approaches find a single solution in about 0.1 millisecond. Our approach provides 2 orders of magnitude more solutions in only one order of magnitude more time. Figure 4 also demonstrates that the approach scales linearly with number of requested solution samples. The gradient of the increase is low

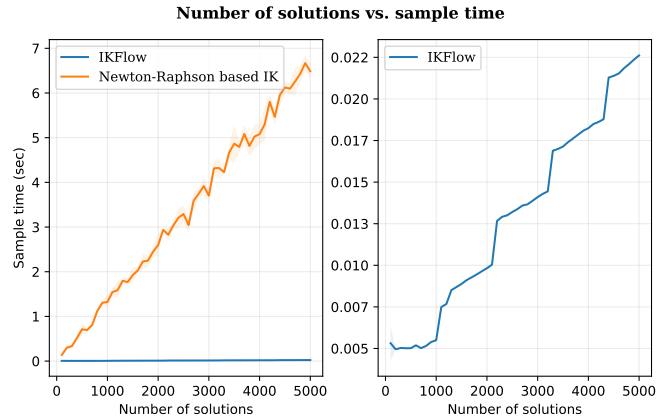


Fig. 4: The run time of the IKFlow model and of a traditional Newton-Raphson optimization based IK solver for ATLAS as a function of the number of requested solutions. The transparent background for each plot indicates the standard deviation of the sample time for a given IK number of requested solutions. The relationship for the IKFlow model is linear after an initial flat spot. Since the model is sampled on the GPU, thousands of solutions can be sampled in under 15 milliseconds. The IKFlow models for the other robots have similar runtime curves, but shifted vertically up or down depending on the number of coupling layers.

with 4,000 samples found in just under 20 milliseconds. This means that even complex solution sets can be approximated quickly. For another point of comparison, if a nonlinear optimization is fed random seeds in hopes that the local minima it finds are different it takes more than a second to return 1,000 samples.

C. Solution Space Coverage

Figure 3 provides a qualitative comparison of rejection sampled solution sets with solution sets from IKFlow. The solution spaces look quite similar, and provide reference points for the MMD score for other chains. All of the kinematic chains included have a MMD score under 0.05. This implies that the IKFlow solution spaces are very similar to the rejection sampled solution spaces, with only a few erroneous solutions,

Robot	DOF	MMD Score	Time (msec)	Average L2 Position Error (millimeters)	Avg Angular Error (degrees)
ATLAS (2013) - Arm and Waist	9	0.0372	4.79	2.66	0.61
ATLAS (2013) - Arm and Waist	6	0.0046	6.4	1.19	0.28
Panda	7	0.0304	6.64	7.75	2.82
Robonaut 2 - Arm and Waist	8	0.0375	6.44	6.33	1.24
Robonaut 2 - Arm	7	0.0325	6.46	1.92	0.46
Valkyrie - Whole Arm and Waist	10	0.0374	8.57	3.5	0.74
Valkyrie - Lower Arm	4	3.25×10^{-6}	4.87	0.36	0.15
Valkyrie - Whole Arm	7	0.0295	6.47	1.62	0.37

TABLE II: This table contains the results of the experimental runs. The MMD Score is the average of 1000 Maximum Mean Discrepancy scores, each computed between a set of 250 solutions found through rejection sampling, and a set of solutions of equal size returned by IKFlow for a randomly drawn pose. The MMD score, when low, implies that two distributions are similar. Since the IKFlow distribution is compared with a ground truth distribution the MMD score provides a measure of how well the solution distribution from the network covers the whole solution space. The minimum value for MMD score is 0, and implies that the distributions are identical. The maximum value for MMD score is 2, and implies there is no similarity between the distributions. Time is the total time to return 100 solutions for one Cartesian pose measured in milliseconds. Average position error and Average angular error are the difference between the desired goal pose and the pose achieved from joint solutions.

or small gaps in coverage.

VI. CONCLUSION

IKFlow is a novel IK solver capable of providing quick, accurate, and diverse solutions for kinematically redundant robots operating in $SE(3)$, based on modeling IK solutions as a distribution over joint poses and using deep generative modeling to model these distributions. Our experiments demonstrated that IKFlow can generate hundreds to thousands of solutions covering the solution space in milliseconds. The average pose error of the results showed that our approach is capable of finding solutions with millimeters of translation error, and less than 1.5 degrees of rotational error. These results demonstrate that IKFlow can serve as the basis for expanded functionality of 7+ DOF kinematic chains.

APPENDIX

A. Model and Training Parameters

The coefficient network depth and width were set to 3 and 1024 respectively. A softflow noise scale of 1×10^{-3} was used across all of the models. The learning rate was set to 5×10^{-4} and decayed exponentially by a factor of γ after every 39000 batches, with γ set to 0.979. The parameters ‘betas’, ‘weight-decay’, and ‘eps’ used by the optimizer were set to (0.95, 0.999), 1.855×10^{-05} , and 1×10^{-4} respectively. Each model was trained until convergence on 2.5 million points using the Ranger optimizer with batch size 128 and the LeakyRELU for the activation function.

REFERENCES

- [1] Ahmed R.J. Almusawi, L. Canan Dülger, and Sadettin Kapucu. A New Artificial Neural Network Approach in Solving Inverse Kinematics of Robotic Arm (Denso VP6242). *Computational Intelligence and Neuroscience*, 2016, 2016. ISSN 16875273. doi: 10.1155/2016/5720163. URL /pmc/articles/PMC5005769/ /pmc/articles/PMC5005769/?report=abstracthttps://www.ncbi.nlm.nih.gov/pmc/articles/PMC5005769/.
- [2] Lynton Ardizzone, Jakob Kruse, Sebastian Wirkert, Daniel Rahner, Eric W. Pellegrini, Ralf S. Klessen, Lena Maier-Hein, Carsten Rother, and Ullrich Köthe. Analyzing inverse problems with invertible neural networks. In *International Conference on Representation Learning*. arXiv, 8 2019. URL https://arxiv.org/abs/1808.04730v3.
- [3] Patrick Beeson and Barrett Ames. TRAC-IK: An open-source library for improved solving of generic inverse kinematics. In *IEEE-RAS International Conference on Humanoid Robots*, volume 2015-December, pages 928–935. IEEE Computer Society, 12 2015. ISBN 9781479968855. doi: 10.1109/HUMANOIDS.2015.7363472.
- [4] Lukas Biewald. Experiment Tracking with Weights and Biases, 2020.
- [5] Akos Csiszar, Jan Eilers, and Alexander Verl. On solving the inverse kinematics problem using neural networks. In *2017 24th International Conference on Mechatronics and Machine Vision in Practice, M2VIP 2017*, volume 2017-December, pages 1–6. Institute of Electrical and Electronics Engineers Inc., 12 2017. ISBN 9781509065462. doi: 10.1109/M2VIP.2017.8211457.
- [6] Hongkai Dai, Gregory Izatt, and Russ Tedrake. Global inverse kinematics via mixed-integer convex optimization. *International Journal of Robotics Research*, 38(12-13):1420–1441, 10 2019. ISSN 17413176. doi: 10.1177/0278364919846512.
- [7] Jacket Demby’S, Yixiang Gao, and G. N. Desouza. A Study on Solving the Inverse Kinematics of Serial Robots using Artificial Neural Network and Fuzzy Neural Network. In *IEEE International Conference on Fuzzy Systems*, volume 2019-June. Institute of Electrical and Electronics Engineers Inc., 6 2019. ISBN 9781538617281. doi: 10.1109/FUZZ-IEEE.2019.8858872.
- [8] Laurent Dinh, David Krueger, and Yoshua Bengio. Nice: Non-linear independent components estimation, 2015.
- [9] Laurent Dinh, Jascha Sohl-Dickstein, and Samy Bengio. Density estimation using Real NVP. 5 2016. URL http://arxiv.org/abs/1605.08803.
- [10] Arthur Gretton, Karsten M. Borgwardt, Malte J. Rasch, Bernhard Schölkopf, and Alexander Smola. A kernel two-sample test. *Journal of Machine Learning Research*, 13(25):723–773, 2012. URL http://jmlr.org/papers/v13/gretton12a.html.
- [11] Hyeongju Kim, Hyeonseung Lee, Woo Hyun Kang, Joun Yeop Lee, and Nam Soo Kim. SoftFlow: Probabilistic Framework for Normalizing Flow on Manifolds. Technical report. URL https://github.com/ANLGBOY/SoftFlow.
- [12] Diederik P. Kingma and Prafulla Dhariwal. Glow: Generative

flow with invertible 1x1 convolutions, 2018.

- [13] George Papamakarios, Eric Nalisnick, Danilo Jimenez Rezende, Shakir Mohamed, and Balaji Lakshminarayanan. Normalizing Flows for Probabilistic Modeling and Inference. 12 2019. URL <http://arxiv.org/abs/1912.02762>.
- [14] Adam Paszke, Sam Gross, Francisco Massa, Adam Lerer, James Bradbury Google, Gregory Chanan, Trevor Killeen, Zeming Lin, Natalia Gimelshein, Luca Antiga, Alban Desmaison, Andreas Köpf Xamla, Edward Yang, Zach Devito, Martin Raison Nabla, Alykhan Tejani, Sasank Chilamkurthy, Qure Ai, Benoit Steiner, Lu Fang Facebook, Junjie Bai Facebook, and Soumith Chintala. PyTorch: An Imperative Style, High-Performance Deep Learning Library. Technical report, 2019.
- [15] Hailin Ren and Pinhas Ben-Tzvi. Learning inverse kinematics and dynamics of a robotic manipulator using generative adversarial networks. *Robotics and Autonomous Systems*, 124: 103386, 2 2020. ISSN 09218890. doi: 10.1016/j.robot.2019.103386.
- [16] Danilo Jimenez Rezende and Shakir Mohamed. Variational inference with normalizing flows, 2016.
- [17] Danilo Jimenez Rezende, George Papamakarios, Sébastien Racanière, Michael S. Albergo, Gurtej Kanwar, Phiala E. Shanahan, and Kyle Cranmer. Normalizing Flows on Tori and Spheres. In *International Conference on Machine Learning*, 2 2020. URL <http://arxiv.org/abs/2002.02428>.
- [18] Dianmu Zhang and Blake Hannaford. IKBT: solving closed-form Inverse Kinematics with Behavior Tree. *Journal of Artificial Intelligence Research*, 65, 11 2017. URL <http://arxiv.org/abs/1711.05412>.